Optimal control applied to a stage-structured cassava mosaic disease model with vector feeding behavior

Article *in* Results in Control and Optimization · January 2025

DOI: 10.1016/j.rico.2025.100522

4 authors:

Eva Lusekelo
The University of Dodoma
13 PUBLICATIONS **66** CITATIONS
SEE PROFILE

Mlyashimbi Helikumi
Mbeya University of Science and Technology .
31 PUBLICATIONS **146** CITATIONS
SEE PROFILE

Salamida Daudi
Nelson Mandela African Institution of Science and Technology
11 PUBLICATIONS **36** CITATIONS
SEE PROFILE

Steady Mushayabasa
University of Zimbabwe
125 PUBLICATIONS **1,624** CITATIONS
SEE PROFILE

Results in Control and Optimization 18 (2025) 100522

Contents lists available at ScienceDirect

Results in Control and Optimization

journal homepage: www.elsevier.com/locate/rico

Optimal control applied to a stage-structured cassava mosaic disease model with vector feeding behavior

Eva Lusekelo [a], Mlyashimbi Helikumi [b], Salamida Daudi [c], Steady Mushayabasa [d,*]

[a] University of Dodoma, College of Natural and Mathematical Sciences, Department of Mathematics, P.O. Box 338, Dodoma, Tanzania
[b] Mbeya University of Science and Technology, Department of Mathematics and Statistics, College of Science and Technical Education, P.O. Box 131, Mbeya, Tanzania
[c] National Institute of Transport, Faculty of Informatics and Technical Education, Department of Education and Mathematics, P. O. Box 705, Dar-es-Salaam, Tanzania
[d] University of Zimbabwe, Department of Mathematics & Computational Sciences, P.O. Box MP 167 Mount Pleasant, Harare, Zimbabwe

ARTICLE INFO

MSC:
35B40
35K57
35Q92
92D30

Keywords:
Cassava mosaic
Whitefly
Mathematical model
Vector preference
Offspring number
Reproduction number

ABSTRACT

Cassava remains Sub-Saharan Africa's second most crucial staple food crop after maize. However, production of sufficient yields is hampered by pests and diseases. In particular, the whitefly (*Bemisia tabaci*) has the potential to reduce expected yields by 50% since it directly damages cassava leaves by feeding on phloem, causing chlorosis and abscission. This study develops a novel mathematical model for cassava mosaic disease that incorporates immature and adult whitefly populations. Additionally, the model includes vector feeding behavior since prior studies have shown that vectors exhibit preferences to settle for either healthy or infected hosts. We determined the offspring number and carried out its sensitivity analysis. Additionally, we carried out an optimal control study on the use of insecticides and plant roguing as disease control measures against cassava mosaic disease. Our results show that vector preference and efficiency of disease control strategies plays an important role in shaping the short and long-term dynamics of cassava mosaic disease, which subsequently impacts the design of its optimal control strategies.

1. Introduction

Cassava is regarded as the world's fourth most important staple food after rice, wheat and maize, and the second most crucial staple food crop after maize for Sub-Saharan Africans [1]. It is estimated that cassava forms part of the diet of more than a billion people worldwide [1]. Apart from being a food source, cassava is now regarded as one of the most important large-scale agricultural crops for use as a bio-fuel and a source of industrial starch [2]. Cassava is one of the versatile crops, it can grow on poor soils, is easily propagated, requires little cultivation, and can tolerate periodic and extended periods of drought [2]. Owing to these attributes, it is now commonly referred to as the "drought, war and famine crop" of the developing world [2].

Despite its versatility, the production of sufficient cassava for consumption and other uses remains one of the major challenges in the developing world [2]. Among several other factors, pest and diseases are some of the highly ranked challenges that results in heavy yield losses [3]. The whitefly *Bemisia tabaci* (*B. tabaci*), arguably one of the most damaging insects in the world, is one of the major agricultural pest groups that cause low productivity of cassava in Africa [3]. It directly damages cassava leaves by feeding on phloem, causing chlorosis and abscission resulting in yield loss by 50% [3].

* Corresponding author.
E-mail addresses: lusekeloe@nm-aist.ac.tz (E. Lusekelo), mhelikumi@yahoo.co.uk (M. Helikumi), daudisalamida81@gmail.com (S. Daudi), steadymushaya@gmail.com (S. Mushayabasa).

https://doi.org/10.1016/j.rico.2025.100522
Received 19 August 2024; Received in revised form 5 November 2024; Accepted 5 January 2025
Available online 9 January 2025

In this paper, we present a mathematical model for cassava mosaic disease (CMD) that incorporates immature stages of the whitefly population, vector preference, and time-dependent disease control strategies. Recently, various mathematical models of plant-virus and plant-vector-virus have been proposed and analyzed to gain insights into effective methods for reduction of disease incidence thereby increasing plant productivity (see, for example [4–15] and the reference therein). The effects of roguing on minimizing disease incidence has been investigated in several plant-virus model and plant-vector-virus models [6,7]. Al Basir et al. [10] employed a system of ordinary differential equations (ODEs) to evaluate the impact of farming awareness based intervention strategies (plant roguing and insecticide spraying) on increasing plant productivity. A couple of researchers have also investigated the feasibility of time dependent controls to eradicate CMD during an outbreak [5,8,12] In a recent study, Sikazwe et al. [4], demonstrated various ways of managing whitefly development in order to control brown streak virus co-infections.

Despite all the studies, a critical aspect of CMD that remains unexplored is the role of vector feeding behavior on disease dynamics. Prior studies have suggest that the settlement of vector population depends on the preference for plant host status (healthy or infected) [16,17]. There is no doubt that this feeding behavior has an impact of disease transmission dynamics. For example, if infected vectors have preference for healthy plants, this increases pathogen spread in both hosts and vectors. Most of the existing models for CMD transmission assume a uniform interaction of vectors and plants, implying an equally likelihood of disease transmission. Another aspect that has also been largely ignored by existing CMD models is to include all immature stages of the whitefly (egg, first instar, second instar, third instar, fourth instar and pupa). As highlighted in a recent study by Adhurya et al. [5], the researchers postulated that ignoring immature stages of the vector population leads to false predictions since at different stages, the development and survival rate of the whitefly differs. Moreover, the efficiency of control strategies across all the stages of the whitefly is not uniform. For example, it is known that insect growth regulators (IGR) are effective against whitefly nymphs and not on adult populations [3]. A few of the studies that have attempted to incorporate immature stages [4,5], lumped all the four nymph stages together. However, other researchers opine that the mortality of first instars is relatively high compared to other instars since they are highly mobile during the first few hours after egg hatching thereby making them more vulnerable to environmental stress factors [18]. Therefore, the development of mathematical models to quantifying the implications of vector's behavior on disease dynamics is desirable.

The rest of the paper is organized as follows. In Section 2, we commence by presenting a mathematical model for the growth of whitefly population. Through this model, we determined the offspring number which accounts for the strength of the whitefly to persist or become extinct. We extended the whitefly population growth model to into a plant-vector-virus model. We computed the reproduction number and performed the bifurcation analysis. We further extended the plant-vector-virus model to incorporate time-dependent intervention strategies (insecticides use and roguing). In Section 3, we present the results and discussions. Finally, a brief discussion is presented in Section 4.

2. Methods

2.1. Modeling the dynamics of growth of the whitefly

We commence by modeling the growth dynamics of whitefly population. Whiteflies have a characteristic life cycle of seven stages: the egg, four nymphal instars, pupa and the adult stage [19]. It is estimated that the cycle takes approximately 19 to 29 days from egg to adult emergence [19]. Let the variables $E(t)$, $N_i(t)$, $P(t)$, and A_W denote the egg population, the four nymphal instar stages ($i = 1, 2, 3, 4$), the pupa, adult population, respectively. The proposed model is based on the following assumptions:

- The life cycle of the vector commences when an adult whitefly A_W deposits eggs on the upper and lower leaf surfaces of plants [19]. Let b be the oviposition rate, ψ and d_E be the egg development and mortality rates, respectively. Since vectors deposit eggs on plant leaves, it seems reasonable to express egg production as a logistic function: $b\left(1 - \frac{E}{K_W}\right)A_W$, where K_W is the maximum egg density per plant [4]. Thus, the dynamics of egg population satisfies the equation:

$$E'(t) = b(T)\left(1 - \frac{E}{K_W}\right)A_W - \psi E - d_E E. \tag{2.1}$$

- Under ideal environmental conditions, it takes 4–10 days for eggs to hatch into the first nymphal stage [20]. The population of nymphs at the first stage decreases either due to mortality rate at the rate d_1, or progression to the second nymphal stage at rate s_1. Thus, the dynamics of the first nymph population satisfies the equation:

$$N_1'(t) = \psi_1 E - s_1 N - d_1 N_1. \tag{2.2}$$

- The population of nymphs at the second, third and fourth stages can be deduced from the equation:

$$N_i'(t) = s_{i-1} N_{i-1} - s_i N_i - d_i N_i, \qquad i = 2, 3, 4, \tag{2.3}$$

  where s_i denotes the maturity from one stage to the next, and d_i is the natural mortality rate.
- Although the pupa stage is sometimes referred to as the fourth nymphal instar, some researchers opine that it is a unique stage from the fourth nymphal instar stage [18]. Based on this assertion, in this work, we have considered this stage as a unique stage from the fourth nymphal instar stage. Thus, the pupa population increases following the maturation of the fourth

nymphal population at the rate s_4. It decreases due to maturation to the adult stage or natural mortality at the rates s_5 and d_5, respectively. Thus, the dynamics of this population can be summarized by:

$$P'(t) = s_4 N_4 - s_5 P - d_5 P. \tag{2.4}$$

- From the pupal stage, white flies progress to the adult stage. Let μ be the mortality rate of the whitefly adult population. It follows that the dynamics of the adult whitefly population are governed by:

$$A_W'(t) = s_5 P - \mu A_W. \tag{2.5}$$

Combining all assumptions leads to the following system of ODEs (A schematic of the model is given in Fig. 1):

$$E'(t) = b\left(1 - \frac{E}{K_W}\right)A_W - \psi E - d_E E, \tag{2.6}$$

$$N_1'(t) = \psi E - s_1 N_1 - d_1 N_1, \tag{2.7}$$

$$N_2'(t) = s_1 N_1 - s_2 N_2 - d_2 N_2, \tag{2.8}$$

$$N_3'(t) = s_2 N_2 - s_3 N_3 - d_3 N_3, \tag{2.9}$$

$$N_4'(t) = s_3 N_3 - s_4 N_4 - d_4 N_4, \tag{2.10}$$

$$P'(t) = s_4 N_4 - s_5 P - d_5 P, \tag{2.11}$$

$$A_W'(t) = s_5 P - \mu A_W. \tag{2.12}$$

Through direct calculation, one can easily verify that the set Ω_V is positively invariant with respect to the system (2.6)–(2.12)

$$\Omega_V = \left\{ \begin{pmatrix} E \\ N_1 \\ N_2 \\ N_3 \\ N_4 \\ P \\ A_W \end{pmatrix} \in \mathbb{R}_+^7 \;\middle|\; \begin{array}{l} 0 \le E \le K_W, \\ 0 \le N_1 \le \dfrac{\psi K_W}{s_1 + d_1}, \\ 0 \le N_2 \le \dfrac{s_1 \psi K_W}{(s_1 + d_1)(s_2 + d_2)}, \\ 0 \le N_3 \le \dfrac{s_1 s_2 \psi K_W}{(s_1 + d_1)(s_2 + d_2)(s_3 + d_3)}, \\ 0 \le N_4 \le \dfrac{s_1 s_2 s_3 \psi K_W}{(s_1 + d_1)(s_2 + d_2)(s_3 + d_3)(s_4 + d_4)}, \\ 0 \le P \le \dfrac{s_1 s_2 s_3 s_4 \psi K_W}{(s_1 + d_1)(s_2 + d_2)(s_3 + d_3)(s_4 + d_4)(s_5 + d_5)}, \\ 0 \le A_W \le \dfrac{s_1 s_2 s_3 s_4 \psi s_5 K_W}{(s_1 + d_1)(s_2 + d_2)(s_3 + d_3)(s_4 + d_4)(s_5 + d_5)\mu}. \end{array} \right\}$$

Thus, system (2.4) with non-negative initial conditions has a unique solution that is non-negative and bounded from above for all $t \ge 0$.

2.1.1. Equilibrium points and the offspring number

Through direct calculations, we have established that model (2.6)–(2.12) admits two stationary points, (i) the trivial equilibrium point and the non-trivial equilibrium point. The trivial equilibrium point is given by $E^0 = N_1^0 = N_2^0 = N_3^0 = N_3^0 = P^0 = A_W^0 = 0$, and it reflects the extinction or absence of the whitefly population. The non-trivial equilibrium point is given by $\mathcal{E}^* = (E^*, N_1^*, N_2^*, N_3^*, N_3^*, P^*, A_W^*)$ with:

$$E^* = \frac{K_W \mu m_0 m_1 m_2 m_3 m_4 m_5 (Q_0 - 1)}{b\psi s_1 s_2 s_3 s_4 s_5}, \qquad N_1^* = \frac{K_W \mu m_0 m_2 m_3 m_4 m_5 (Q_0 - 1)}{b s_1 s_2 s_3 s_4 s_5}, \tag{2.13}$$

$$N_2^* = \frac{K_W \mu m_0 m_3 m_4 m_5 (Q_0 - 1)}{b s_2 s_3 s_4 s_5}, \quad N_3^* = \frac{K_W \mu m_0 m_4 m_5 (Q_0 - 1)}{b s_3 s_4 s_5}, \tag{2.14}$$

$$N_4^* = \frac{K_W \mu m_0 m_5 (Q_0 - 1)}{b s_4 s_5}, \qquad P^* = \frac{K_W \mu m_0 (Q_0 - 1)}{b s_5}, \quad A_W^* = \frac{K_W \mu m_0 (Q_0 - 1)}{b}, \tag{2.15}$$

$$m_0 = \psi + d_E, \qquad m_j = s_j + d_j, \quad j = 1, \ldots, 5,$$

where Q_0 is the basic offspring number and the mathematical expression is:

$$\begin{aligned} Q_0 &= \frac{b\psi s_1 s_2 s_3 s_4 s_5}{\mu m_0 m_1 m_2 m_3 m_4 m_5} \\ &= \left(\frac{b}{\mu}\right)\left(\frac{\psi}{\psi + d_E}\right)\left(\frac{s_1}{s_1 + d_1}\right)\left(\frac{s_2}{s_2 + d_2}\right)\left(\frac{s_3}{s_3 + d_3}\right)\left(\frac{s_4}{s_4 + d_4}\right)\left(\frac{s_5}{s_5 + d_5}\right). \end{aligned} \tag{2.16}$$

The basic offspring number Q_0 is an integral parameter in ecological models that measures the strength of the whitefly to persist or become extinct. In particular, if $Q_0 \le 1$, then the non-trivial equilibrium point vanishes, which implies that whitefly population becomes extinct. However, if $Q_0 > 1$, it follows that the population grows.

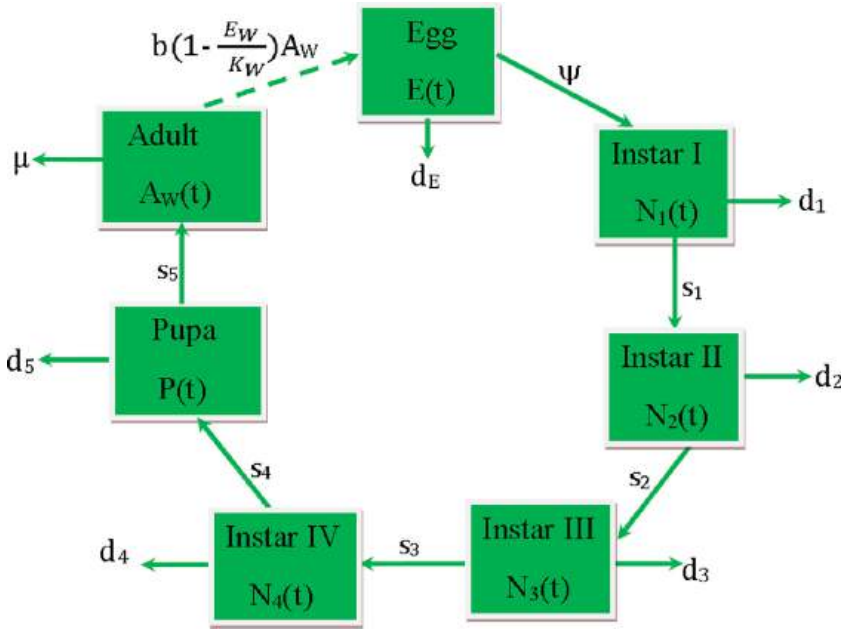

Fig. 1. Model flow diagram summarizing the life cycle of the whitefly. The green rectangular boxes represent the maturity stages: $E(t)$-egg population, $N_1(t)$-First instar, $N_2(t)$- Second instar, $N_3(t)$- Third instar, $N_4(t)$- Fourth instar, $P(t)$- Pupal stage and $A_W(t)$- Adult stage. Solid green connecting boxes represent the development rates from one stage to another. Solid green lines not connecting boxes denote natural mortality. The dotted lines connecting $A_W(t)$ and $E(t)$ denote adult egg laying rate. (For interpretation of the references to color in this figure legend, the reader is referred to the web version of this article.)

The basic offspring number $\mathcal{Q}_0$ deserves a biological interpretation. Observe that $1/\mu$ is the average life span of the adult female whitefly, and $\frac{b}{\mu}$ represents the average number of eggs produced by a female whitefly during its entire lifespan. Of these eggs, only a proportion $\frac{\psi}{\psi + d_E}$ hatches to the first nymphal instar stage. The first nymphal instar population has a probability $\frac{s_1}{s_1 + d_1}$ to survive this stage and become second nymphal instars. Similarly, the probability of nymphs surviving the second, third and fourth stages till they reach the pupa stage are $\frac{s_2}{s_2 + d_2}$, $\frac{s_3}{s_3 + d_3}$ and $\frac{s_4}{s_4 + d_4}$, respectively. The probability of the whitefly surviving the pupal stage and becoming adults is equivalent to $\frac{s_5}{s_5 + d_5}$. Overall, $\mathcal{Q}_0$ is related to the number of eggs laid by a single whitefly, the probability that eggs are hatched into nymps, the survival probability of the nymphs at each stage, and the survival probability of the whitefly at the pupal stage. Based on this relation, one can observe that ideal environment conditions are of utmost importance to understand the dynamics of whiteflies and their transmission of diseases.

2.2. Sensitivity analysis of $\mathcal{Q}_0$

Based on $\mathcal{E}^*$, we have observed that the growth and extinction of the whitefly population depends on the basic offspring number $\mathcal{Q}_0$. When $\mathcal{Q}_0 \leq 1$, the population becomes extinct and it persists whenever $\mathcal{Q}_0 > 1$. Therefore, it is imperative to identify model parameters that are strongly correlated to $\mathcal{Q}_0$. To investigate this relationship, we carried out sensitivity analysis using the Latin hypercube sampling (LHS) technique and the partial rank correlation coefficients (PRCC) method. According to Gao et al. [21], a PRCC provides a global sensitivity analysis for nonlinear but monotone relationships between inputs and outputs.

We adapted parameter values and ranges from published peer-reviewed articles (see ., Table 1). In particular, prior studies suggest that under optimal environmental conditions, an adult female whitefly is capable of laying a maximum of 387 eggs for its entire life span which ranges between 30–40 days [18]. Based on this assertion, we set $\mu = 1/30$ and $b = 387/30$. Experimental and field studies also suggest that the whitefly life cycle takes: 6–10 days for egg hatch, 4–10 days as a first instar nymph, 3–7 days as second instar nymph, 4–5 days as third instar nymph, 4–5 days as fourth instar nymph and 6–10 days for the pupa [20]. The mortality of cassava whitefly can be categorized into several classes such as dislodgement, predation, parasitism (for nymphs only), unknown death, and inviability (for eggs only) [22]. Furthermore, prior studies suggest that the mortality of egg and frst instar stages is relatively higher than all other stages [18]. In particular, it is well known that first instars are highly mobile during the first few hours after egg hatching making them more vulnerable to environmental stress factors [18].

Fig. 2 depict the PRCCs between the parameters and offspring number. We can observe that increasing the oviposition rate significantly increases the offspring number while an increase in mortality rates of both immature and adult whitefly populations significantly reduces the offspring number. This implies that efforts to reduce the whitefly population should be aimed at increasing the mortality rates, particularly of the adult population.

Table 1
Interpretation of model parameters and their baseline values adopted from literature.

Symbol	Biological definition	Unit	Baseline value	Source
b	Oviposition rate	Eggs laid per day	387/31	[18]
ψ	Egg development duration	days	7.2 (6–10)	[20]
s_1	First instar development duration	days	7.5 (4–10)	[20]
s_2	Second instar development duration	days	4.7 (3–7)	[20]
s_3	Third instar development duration	days	4 (4–5)	[20]
s_4	Fourth development duration	days	4 (3–4)	[20]
s_5	Pupal development duration	days	10 (6–10)	[20]
d_E, d_1	Mortality rate of egg and first instar stages	day^{-1}	0.12	[4]
d_2, d_3, d_4, d_5	Mortality of 2nd, 3rd 4th instar stages, repectively	day^{-1}	0.012	[4]
d_5	Mortality of pupa stages, repectively	day^{-1}	0.012	[4]
μ	Mortality rate of adult whitefly	day^{-1}	0.03	[4]
K_W	Maximum egg density per plant	egg per $plant^{-1}$	5000	[4]

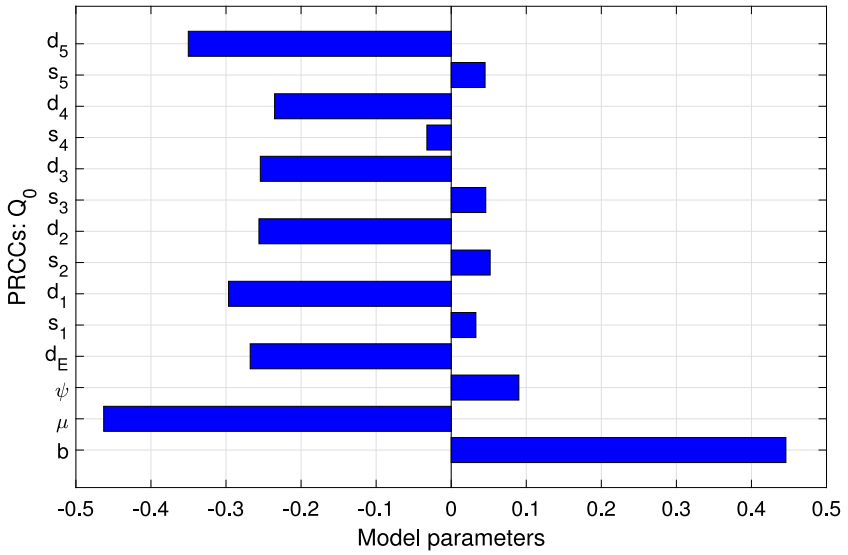

Fig. 2. Sensitivity analysis of $\mathcal{Q}_0$.

2.3. Modeling transmission dynamics of the cassava mosaic disease

Whiteflies are infected with the disease upon feeding on an infected plant host. Infected whiteflies will the spread the disease when they feed on cassava leaves. It is worth noting that just like adults, nymphs have sucking mouthparts to pierce the leaf tissue and consume phloem sap [23], hence they are capable of transmitting the disease. However, in this study we ignored their contribution since prior studies suggests that their contribution to disease dynamics is extremely minimal due to low mobility [24].

Moreover, prior studies suggest that CMD is not a transovarial disease [25]. Based on these assumptions, in this section, we propose a new framework for CMD that incorporates the interaction of the plant host and whitefly. We are cognizant that if $\mathcal{Q}_0 < 1$, the whitefly population will become extinct, thus the proposed model considers $\mathcal{Q}_0 > 1$, and that the whitefly population is at the equilibrium $\mathcal{E}^*$. To account for disease transmission in adult whitefly, we subdivide the adult whitefly population into two compartments, U and V, representing susceptible and infected, respectively. Thus, the total adult whitefly population is $A_W^* = U+V$. Meanwhile, let $S(t)$, $L(t)$ and $I(t)$ be the numbers of healthy, latent infected and infectious plants, respectively, at time t.

It is well documented that pathogen prevalence in vector-borne diseases (VBDs) generally depends on vector behavioral dynamics. In particular, it has been established that vectors have different preference weights when selecting hosts [16,17]. Recent studies have shown that vectors have heterogeneous feeding behavior for infected or healthy hosts, which significantly impacts the spread of infection [16,17]. To account for this behavior, we introduced the parameters p_1 and p_2, which are defined as the probabilities that an adult whitefly arrives on a plant at random and picks the plant that is non-infectious (susceptible and latent) and infectious, respectively [17]. The higher the probability, the higher the preference weight. Thus, the likelihood of an adult whitefly to chose a non-infectious plant is $\dfrac{p_1 S}{p_1(S+L)+p_2 I}$, and the probability of an adult whitefly selecting an infectious plant is $\dfrac{p_2 I}{p_1(S+L)+p_2 I}$. Therefore, the number of newly occurring infections in plant population per unit time at time t be:

$$\beta_{VH}\frac{p_1 S}{p_1(S+L)+p_2 I}V = \beta_{VH}\frac{p_1 S}{p_1(S+L)+(1-p_1)I}V, \tag{2.17}$$

since $p_1 + p_2 = 1$. In (2.17), parameter β_{VH} models the rate of transfer of infection from an adult infectious whitefly vector to a susceptible plant. Similarly, the population of newly generated adult whitefly per unit time at time t is $\beta_{HV}\frac{p_2 I}{p_1(S+L)+(1-p_1)I}U$, where β_{HV} is the transmission coefficient accounting for disease transfer from an infectious plant to a susceptible adult whitefly. Thus, our new plant-vector model incorporating vector preference is given by:

$$\left.\begin{aligned}
\frac{dU}{dt} &= \frac{K_W\mu(\psi+d_E)(Q_0-1)}{b} - \frac{\beta_{HV}(1-p_1)IU}{p_1(S+L)+(1-p_1)I} - \mu U,\\
\frac{dV}{dt} &= \frac{\beta_{HV}(1-p_1)IU}{p_1(S+L)+(1-p_1)I} - \mu V,\\
\frac{dS}{dt} &= rS\left(1-\frac{S+L+I}{K_H}\right) - \frac{\beta_{VH}p_1VS}{p_1(S+L)+(1-p_1)I} - hS,\\
\frac{dL}{dt} &= \frac{\beta_{VH}p_1VS}{p_1(S+L)+(1-p_1)I} - (\alpha+h)L,\\
\frac{dI}{dt} &= \alpha L - (h+g)I,
\end{aligned}\right\} \tag{2.18}$$

where β_{HV} is the transmission coefficient from plant host to susceptible whitefly, r is the rate of replanting of healthy plants, K_H is the plant density, β_{VH} is the transmission coefficient from a vector to a plant host, α is the rate of progression of latent infected plants to the infectious state, h is the harvesting rate, and g models plant loss/rouging. It can be easily verified that the domain of biological interest:

$$\Omega_{VH} = \left\{(U,V,S,L,I)\in\mathbb{R}^5_+ :\ U+V = A^*_W,\ S+L+I\le K_H\right\}, \tag{2.19}$$

is positively invariant and attracting all orbits with respect to the model (2.18). The disease-free equilibrium (DFE) for model (2.18) is:

$$\mathcal{W}^0 : (U^0,V^0,X^0,Y^0) = \left(\frac{K_W(\psi+d_E)(Q_0-1)}{b}, 0, K_H, 0, 0\right). \tag{2.20}$$

The basic reproduction number near the DFE can defined using the next generation matrix (NGM) [26]. Based on the NGM, it follows that the non-negative matrix $\mathcal{F}$ that denotes the generation of new infection and the non-singular matrix $\mathcal{V}$ that denotes the disease transfer among compartments, are respectively given by (evaluated at DFE) :

$$\mathcal{F} = \begin{bmatrix} 0 & 0 & \frac{\beta_{HV}K_V(\psi+d_E)(Q_0-1)}{b}\\ \beta_{VH}K_H & 0 & 0\\ 0 & 0 & 0 \end{bmatrix}, \quad \text{and} \quad \mathcal{V} = \begin{bmatrix} \mu & 0 & 0\\ 0 & \alpha+h & 0\\ 0 & -\alpha & g+h \end{bmatrix}. \tag{2.21}$$

From (2.21), it follows that the reproduction number of model (2.18) is:

$$\mathcal{R}_0 = \sqrt{\frac{\beta_{HV}\beta_{VH}}{K_H}\frac{(1-p_1)}{p_1}\frac{\alpha}{(\alpha+h)(g+h)}K_E\frac{(\psi+d_E)}{b}(Q_0-1)}. \tag{2.22}$$

The reproduction number $\mathcal{R}_0$ represents the average number of new cases (hosts or vectors) generated in a wholly susceptible population, by one infectious individual (host or adult whitefly, respectively) during its entire infectious period. We can observe that $\mathcal{R}_0$ makes biological sense whenever $Q_0 > 1$. The term $\frac{\alpha}{(\alpha+h)}$ represents the probability that a plant will survive the exposed state to become infectious, $\frac{1}{(g+h)}$ is the average infectious lifetime of the plant, $\frac{(1-p_1)}{p_1}$ is the ratio of non-infectious to infectious plants.

2.4. Effects of vector feeding behavior on disease transmission potential

In this subsection, we makes use of the parameter values in Table 2 and the expression (2.22) to examine the influence of vector feeding behavior, offspring number and infection rate on the disease transmission potential (Figs. 3 and 4). Figs. 3(a) and 3(b) illustrate the effect of varying vector feeding preference for different offspring numbers. In Fig. 3(a), we can observe that when the offspring number is 200 and at least 40% of adult susceptible whitefly prefers to feed on healthy plants, then the disease will die out, otherwise it will persist. Similarly, in Fig. 3(b), we can note that if the offspring number is increased from 200 to 500, then for the disease to become extinct, at least 60% of the susceptible adult whitefly population should have preference to feed on plants with similar status. Overall, we can deduce that, if vectors exhibit a preference for host with the opposite infection status then the disease transmission potential increases significantly (Fig. 4). In Fig. 3(c) we can also observe that disease transmission potential is also significantly affected by disease transmission rates. When disease transmission rates are high ($\beta_{VH} = \beta_{HV} = 0.25$) and the offspring number is 500, then the disease may die out if almost 100% of the vectors exhibit preference for hosts with similar infection status.

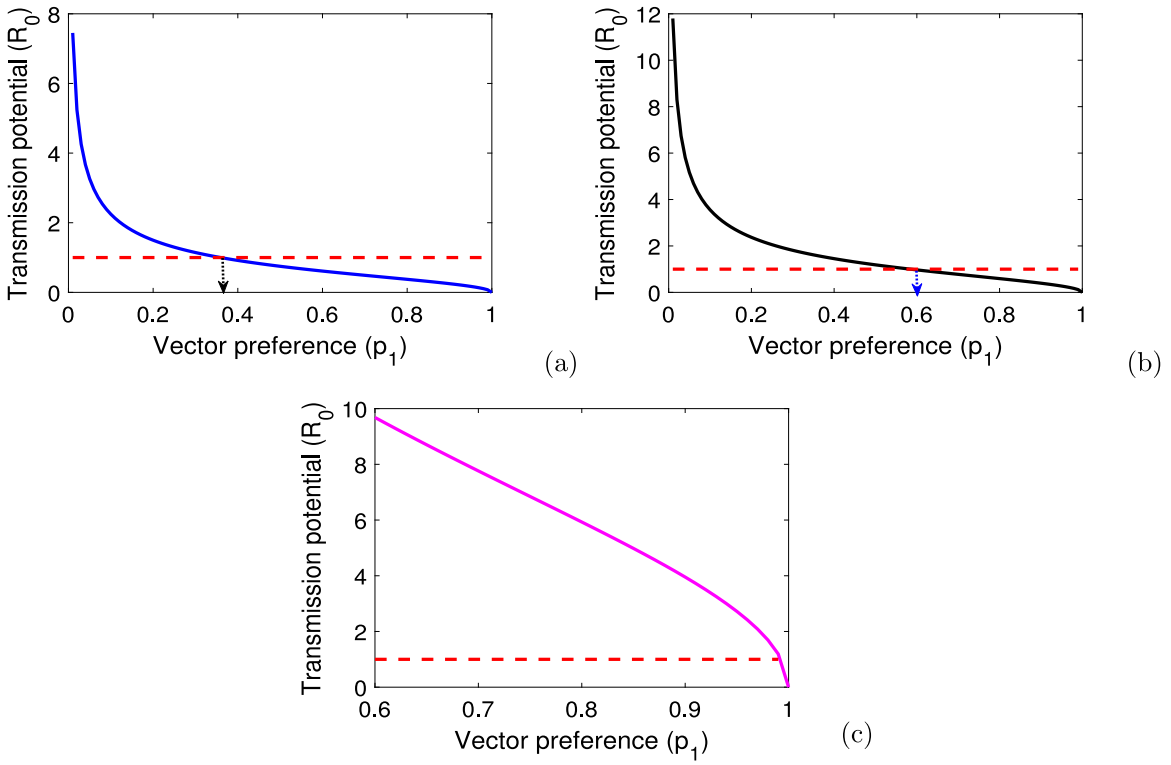

Fig. 3. Simulation results showing the effects of vector preference on disease transmission potential ($\mathcal{R}_0$): we set (a) $\mathcal{Q}_0 = 200$, $\beta_{VH} = \beta_{HV} = 0.025$ (b) $\mathcal{Q}_0 = 500$, $\beta_{VH} = \beta_{HV} = 0.025$ (c) $\mathcal{Q}_0 = 500$, $\beta_{VH} = \beta_{HV} = 0.25$.

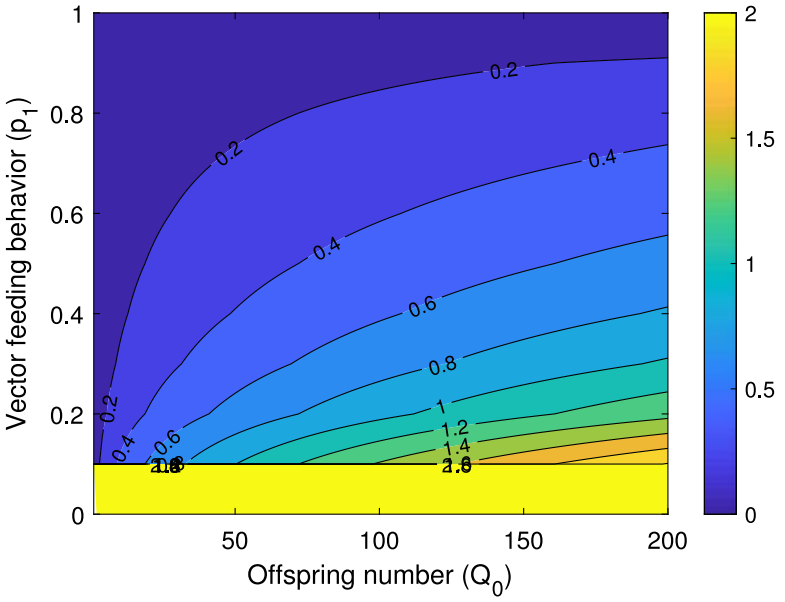

Fig. 4. A contour plot showing the influence of the offspring number ($\mathcal{Q}_0$) and vector feeding behavior (p_1) on disease transmission potential.

Table 2
Interpretation of model parameters and their baseline values adopted from literature.

Symbol	Biological definition	Unit	Baseline value	Source
K_H	Maximum plant density	plants per area	10,000	[4]
β_{VH}	Transmission coefficient from vector to plant	vector^{-1} day^{-1}	0.0025 (0.002–0.5)	[4]
β_{HV}	Transmission coefficient from plant to vector	plant^{-1}day^{-1}	0.0025 (0.002–0.5)	[4]
α	Plant incubation rate	day^{-1}	0.035 (0–1)	[14]
p_1	Probability that a whitefly arrives at plant at random and picks the plant which is non-infectious	dimensionless	0.5 (0–1)	
r	Growth rate of plant	day^{-1}	0.1 (0.025–0.5)	[15]
g	Plant roguing	day^{-1}	0.033 (0–0.033)	[15]
h	Harvesting rate	day^{-1}	0.003 (0.002–0.004)	[15]

Table 3
Number of possible positive real roots of (2.23) for $\mathcal{R}_0 < 1$ and $\mathcal{R}_0 > 1$.

Case	a_0	a_1	a_2	$\mathcal{R}_0$	No. of sign changes	No. of possible positive real roots
1	+	+	+	$\mathcal{R}_0 < 1$	0	0
2	+	+	−	$\mathcal{R}_0 > 1$	1	1
3	+	−	+	$\mathcal{R}_0 < 1$	2	0, 2
4	+	−	−	$\mathcal{R}_0 > 1$	1	1

2.5. Bifurcation analysis

In order to investigate the long-term dynamics of CMD, we investigate the existence of the endemic equilibrium point. For this section alone, disease transmission follows the mass action principle as in [8,10–12]. Furthermore, it also worth noting that $\frac{\beta_{HV}(1-p_1)IU}{p_1(S+L)+(1-p_1)I} \leq \beta_{HV} IU$ and $\frac{\beta_{VH} p_1 VS}{p_1(S+L)+(1-p_1)I} \leq \beta_{VH} p_1 VS$ for all $t \geq 0$. Thus, solving system (2.18) excluding the third equation in terms of $I = I^{**}$ leads to:

$$U^{**} = \frac{K_W \mu m_0(Q_0-1)}{b(\mu+\beta_{HV} I^{**})}, \qquad V^{**} = \frac{\beta_{HV} K_W m_0(Q_0-1) I^{**}}{b(\mu+\beta_{HV} I^{**}),}$$
$$S^{**} = \frac{b(\alpha+h)(g+h)(\mu+\beta_{HV} I^{**})}{\alpha\beta_{HV}\beta_{VH} K_W m_0(Q_0-1)}, \qquad L^{**} = \frac{(g+h)I^{**}}{\alpha},$$

and I^{**} is determined by:

$$a_0 I^2 + a_1 I + a_2 = 0, \tag{2.23}$$

where:

$$a_0 = \frac{b^2(r-h)(g+h)^2(\alpha+h)^2}{K_H K_W^2 m_0^2(Q_0-1)^2\alpha^2\beta_{VH}^2}\left(1+\frac{(g+h+\alpha)}{(g+h)(\alpha+h)}\frac{\beta_{VH} K_W m_0(Q_0-1)}{b}\right) > 0,$$
$$a_1 = \frac{(g+h)(\alpha+h)}{\alpha}\left(1+\frac{2(g+h)(\alpha+h)(r-h)\mu b^2}{K_H K_W^2 m_0^2(Q_0-1)^2\alpha^2\beta_{VH}^2\beta_{HV}}\right)$$
$$+\frac{(g+h)(\alpha+h)(r-h)(\alpha+g+h)b^2}{K_H K_W^2 m_0^2(Q_0-1)^2\beta_{VH}^2\beta_{HV}}\left(1-\frac{\beta_{HV} K_H}{\mu}\frac{\alpha}{(\alpha+g+h)}\right),$$
$$a_2 = \frac{(r-h)(g+h)^2(\alpha+h)^2\mu^2}{K_H K_W^2 m_0^2(Q_0-1)^2\alpha^2\beta_{VH}^2\beta_{HV}^2}(1-\mathcal{R}_0).$$

We can observe that the number of possible positive real roots the polynomial depend on the signs of a_1 and a_2. Furthermore, one can observe whenever $\mathcal{R}_0 < 1$, it follows that $a_2 > 0$ since $\frac{\beta_{HV} K_H}{\mu}\frac{\alpha}{(\alpha+g+h)} < 1$. Making use of the Descartes rule of signs on the quadratic equation, we list the various possibilities for the roots of (2.23) in Table 3.

Based on this analysis, we can conclude that the only possibilities are 1, 2 and 4 this leads to the following results:

Theorem 2.1. *The model (2.18) admits:*
(i) No endemic equilibrium if $\mathcal{R}_0 < 1$, and cases 1 holds.
(ii) A unique endemic equilibrium $\mathcal{E}^*$ if $\mathcal{R}_0 > 1$ when cases 2 and 4 are satisfied;

To support Theorem 2.1, we perform the bifurcation analysis of model (2.18) making use of the center manifold theorem presented in [27]. This technique entails investigating the dynamical behaviors of model (2.18) near $\mathcal{W}^0$ and parameter values

around $\mathcal{R}_0 = 1$ being governed by Eq. (2.24):

$$u'(t) = au^2 + bu\mu + \mathcal{O}(u^3), \tag{2.24}$$

where μ is the bifurcation parameter, u is the center manifold of system (2.18) at $\mathcal{R}_0 = 1$. We now redefine transmission coefficients as follows; $\beta_{VH} = \theta p_{VH}$ and $\beta_{HV} = \theta p_{HV}$, where θ is the whitefly feeding rate and p_{VH} denotes the probability of infection when an adult infectious whitefly feeds on a susceptible plant. Similarly, p_{HV} represents the probability of infection of a susceptible adult whitefly when it feeds on an infectious host. Thus, in this section, we set our bifurcation parameter as $\mu = \theta$. Furthermore, the expression of a and b will be derived in the following discussion. We focus on the simple zero eigenvalue for $D_x f(x_0, \phi)|_{\mathcal{R}_0=1}$, and the corresponding left and right eigenvectors v and w, such that $vw = 1$, with w and v given by:

$$v = \begin{pmatrix} 0 & \dfrac{\theta p_{VH}\alpha K_H}{\mu(\alpha+h)} & 0 & \dfrac{\alpha}{\alpha+h} & 1 \end{pmatrix}, \tag{2.25}$$

and:

$$w = \begin{pmatrix} -\dfrac{\theta p_{HV} K_W m_0(\mathcal{Q}_0-1)}{b} \\ \dfrac{\theta p_{HV} K_W m_0(\mathcal{Q}_0-1)}{b} \\ -\dfrac{r}{r+h} - \dfrac{\theta^2 p_{HV} p_{VH} K_H (r+\alpha+h)}{\mu(r+h)(\alpha+h)} \dfrac{K_W m_0(\mathcal{Q}_0-1)}{b} \\ \dfrac{\theta^2 p_{HV} p_{VH} K_W m_0(\mathcal{Q}_0-1)}{b(\alpha+h)} \\ 1 \end{pmatrix}. \tag{2.26}$$

Then, we compute the second-order partial derivatives of f for $\dfrac{\partial^2 f_i(x_0,\phi)}{\partial x_j \partial x_k}|_{\mathcal{R}_0=1}$ and $\dfrac{\partial^2 f_i(x_0,\phi)}{\partial x_j \partial \mu}|_{\mathcal{R}_0=1}$. The non-zero elements are presented in Eq. (2.27)

$$\left.\begin{aligned}
&\frac{\partial^2 f_1(x_0,\phi)}{\partial x_1 \partial x_5}|_{\mathcal{R}_0=1} = \frac{\partial^2 f_1(x_0,\phi)}{\partial x_5 \partial x_1}|_{\mathcal{R}_0=1} = -\theta p_{HV}, \quad \frac{\partial^2 f_2(x_0,\phi)}{\partial x_1 \partial x_5}|_{\mathcal{R}_0=1} = \frac{\partial^2 f_2(x_0,\phi)}{\partial x_5 \partial x_1}|_{\mathcal{R}_0=1} = \theta p_{HV}, \\
&\frac{\partial^2 f_3(x_0,\phi)}{\partial x_2 \partial x_3}|_{\mathcal{R}_0=1} = \frac{\partial^2 f_3(x_0,\phi)}{\partial x_3 \partial x_2}|_{\mathcal{R}_0=1} = -\theta p_{VH}, \quad \frac{\partial^2 f_4(x_0,\phi)}{\partial x_2 \partial x_3}|_{\mathcal{R}_0=1} = \frac{\partial^2 f_4(x_0,\phi)}{\partial x_3 \partial x_2}|_{\mathcal{R}_0=1} = \theta p_{VH}, \\
&\frac{\partial^2 f_3(x_0,\phi)}{\partial x 3 \partial x_3}|_{\mathcal{R}_0=1} = -\frac{2r}{K_H}, \quad \frac{\partial^2 f_3(x_0,\phi)}{\partial x_3 \partial x_4}|_{\mathcal{R}_0=1} = \frac{\partial^2 f_3(x_0,\phi)}{\partial x_4 \partial x_3}|_{\mathcal{R}_0=1} = -\frac{r}{k_H}, \\
&\frac{\partial^2 f_3(x_0,\phi)}{\partial x_4 \partial x_5}|_{\mathcal{R}_0=1} = \frac{\partial^2 f_3(x_0,\phi)}{\partial x_5 \partial x_4}|_{\mathcal{R}_0=1} = -\frac{r}{K_H}, \quad \frac{\partial^2 f_1(x_0,\phi)}{\partial x_5 \partial \theta}|_{\mathcal{R}_0=1} = -\frac{K_V p_{HV} \mu m_0(\mathcal{Q}_0-1)}{b}, \\
&\frac{\partial^2 f_2(x_0,\phi)}{\partial x_5 \partial \theta}|_{\mathcal{R}_0=1} = \frac{K_W p_{HV} \mu m_0(\mathcal{Q}_0-1)}{b}, \quad \frac{\partial^2 f_3(x_0,\phi)}{\partial x_2 \partial \theta}|_{\mathcal{R}_0=1} = -K_H p_{VH}, \\
&\frac{\partial^2 f_4(x_0,\phi)}{\partial x_2 \partial \theta}|_{\mathcal{R}_0=1} = K_H p_{VH}.
\end{aligned}\right\} \tag{2.27}$$

Utilizing formulas and results in [27], we compute a and b as presented in (2.28):

$$\left.\begin{aligned}
a &= \frac{1}{2}\sum_{i,jk=1}^{5} v_i w_j w_k \frac{\partial^2 f_i(x_0,\phi)}{\partial x_j \partial x_k}|_{\mathcal{R}_0=1} \\
&= -\frac{K_W \theta^2 p_{VH} p_{HV} \alpha K_H m_0(\mathcal{Q}_0-1)}{b(\alpha+h)} \left[p_{HV} + \left(\frac{\theta^3 p_{HV}^2 p_{VH} K_H \alpha r(r+\alpha+h)}{(\alpha+h)(r+h)^2} \right) \frac{K_W m_0(\mathcal{Q}_0-1)}{b} \right], \\
b &= \sum_{i,jk=1}^{5} v_i w_j \frac{\partial^2 f_i(x_0,\phi)}{\partial x_j \partial \theta}|_{\mathcal{R}_0=1} \\
&= \frac{K_W m_0 \theta \alpha p_{VH} K_H (1+p_{HV})(\mathcal{Q}_0-1)}{b(\alpha+h)}.
\end{aligned}\right\} \tag{2.28}$$

We can observe that when $\mathcal{Q}_0 > 1$, $a < 0$ and $b > 0$ and it implies that model (2.18) admits a forward bifurcation at $\mathcal{R}_0 = 1$, as illustrated graphically in Fig. 5. Based on this result, we have the following theorem:

Theorem 2.2. *At $\mathcal{R}_0 = 1$, model (2.18) admits a forward bifurcation.*

2.6. Optimal control

Insecticide use and the removal of infected plants from the field (roguing) are some of the commonly used strategies to control the spread of CMD. In this section, we seek to investigate the cost effectiveness of mitigating the two aforementioned strategies. Thus, we propose the objective functional (2.29):

$$J(c,g) = \int_0^{t_f} \left[L(t) + I(t) + V(t) + U(t) + P(t) + E(t) + \sum_{i=1}^{4} N_i(t) + \frac{B_1 c^2(t)}{2} + \frac{B_2 g^2(t)}{2} \right] dt, \tag{2.29}$$

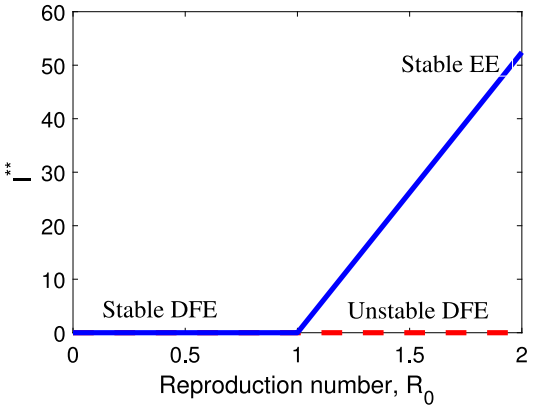

Fig. 5. Bifurcation diagram of model (2.18) showing the existence of a forward bifurcation at $\mathcal{R}_0 = 1$, with the bifurcation parameter $\theta = 2.5 \times 10^{-7}$ and all other parameter values are as in Table 2.

subject to system (2.30)–(2.40):

$$E'(t) = b\left(1 - \frac{E}{K_W}\right)(U+V) - \psi E - d_E E, \tag{2.30}$$

$$N_1'(t) = \psi E - s_1 N_1 - d_1 N_1 - \epsilon_1 c(t) N_1, \tag{2.31}$$

$$N_2'(t) = s_1 N_1 - s_2 N_2 - d_2 N_2 - \epsilon_1 c(t) N_2, \tag{2.32}$$

$$N_3'(t) = s_2 N_2 - s_3 N_3 - d_3 N_3 - \epsilon_1 c(t) N_3, \tag{2.33}$$

$$N_4'(t) = s_3 N_3 - s_4 N_4 - d_4 N_4 - \epsilon_1 c(t) N_4, \tag{2.34}$$

$$P'(t) = s_4 N_4 - \gamma P - d_P P, \tag{2.35}$$

$$U'(t) = \gamma P - \frac{\beta_{HV}(1-p_1) I U}{p_1(S+L) + (1-p_1) I} - \mu U - \epsilon_2 c(t) U, \tag{2.36}$$

$$V'(t) = \frac{\beta_{HV}(1-p_1) I U}{p_1(S+L) + (1-p_1) I} - \mu V - \epsilon_2 c(t) V, \tag{2.37}$$

$$S'(t) = rS\left(1 - \frac{S+L+I}{K_H}\right) - \frac{\beta_{VH} p_1 V S}{p_1(S+L) + (1-p_1) I} - hS, \tag{2.38}$$

$$L'(t) = \frac{\beta_{VH} p_1 V S}{p_1(S+L) + (1-p_1) I} - (\alpha + h) L, \tag{2.39}$$

$$I'(t) = \alpha L - hI - \epsilon_3 g(t) I, \tag{2.40}$$

where the constants B_1 and B_2 represent the weight associated with control variables $c(t)$ (insecticide application) and $g(t)$ (roguing), respectively. Moreover, ϵ_1 and ϵ_2 represent the efficiency of insecticide use to reduce immature and mature whitefly population, respectively. Similarly, ϵ_3 accounts for the efficiency of plant rouging. Our optimal control problem seek to determine a sect of controls capable of minimizing the infected plant population as well as the total vector population at minimal cost of implementing controls c and g. Let c^* and g^* be the optimal controls. We desire to determine a set of control functions such that:

$$J(c^*, g^*) = \min J(c, g), \qquad (c, g) \in \mathcal{W}, \tag{2.41}$$

subject to system (2.30)–(2.40), where $\mathcal{W}$ is the set of measurable function defined from $[0, t_f]$ to $[0, 1]$. Making use of the Pontryagin's maximum Principle [28], we have the Hamiltonian function H(2.42):

$$\begin{aligned} H = {} & L + I + V + U + P + E + \sum_{i=1}^{4} N_i + \frac{1}{2}(B_1 c^2(t) + B_2 g^2(t)) \\ & + \lambda_1 E'(t) + \lambda_2 N_1'(t) + \lambda_3 N_2'(t) + \lambda_4 N_3'(t) + \lambda_5 N_4'(t) + \lambda_6 P'(t) \\ & + \lambda_7 U'(t) + \lambda_8 V'(t) + \lambda_9 L'(t) + \lambda_{10} I'(t), \end{aligned} \tag{2.42}$$

where λ_j, $j = 1, 2, \ldots, 10$ are the adjoint variables satisfying the adjoint system (2.43)–(2.53):

$$\frac{d\lambda_1}{dt} = -\frac{\partial H}{\partial E}$$

$$= -1 + \left(\frac{bU}{K_W} + \psi + d_E\right)\lambda_1 - \psi\lambda_2, \tag{2.43}$$

$$\frac{d\lambda_2}{dt} = -\frac{\partial H}{\partial N_1}$$

$$= -1 + (\epsilon_1 c(t) + d_1 + s_1)\lambda_2 - s_1\lambda_3, \tag{2.44}$$

$$\frac{d\lambda_3}{dt} = -\frac{\partial H}{\partial N_2}$$

$$= -1 + (\epsilon_1 c + d_2 + s_2)\lambda_3 - s_2\lambda_4, \tag{2.45}$$

$$\frac{d\lambda_4}{dt} = -\frac{\partial H}{\partial N_3}$$

$$= -1 + (\epsilon_1 c + d_3 + s_3)\lambda_4 - s_3\lambda_5, \tag{2.46}$$

$$\frac{d\lambda_5}{dt} = -\frac{\partial H}{\partial N_4}$$

$$= -1 + (\epsilon_1 c + d_4 + s_4)\lambda_5 - s_4\lambda_6, \tag{2.47}$$

$$\frac{d\lambda_6}{dt} = -\frac{\partial H}{\partial P}$$

$$= -1 + d_P\lambda_6 - \gamma\lambda_7, \tag{2.48}$$

$$\frac{d\lambda_7}{dt} = -\frac{\partial H}{\partial U}$$

$$= -1 - b\left(1 - \frac{E}{K_V}\right)\lambda_1 + (\epsilon_2 c + \mu)\lambda_7 + \frac{\beta_{HV}(1-p_1)I}{p_1(S+L)+(1-p_1)I}(\lambda_7 - \lambda_8), \tag{2.49}$$

$$\frac{d\lambda_8}{dt} = -\frac{\partial H}{\partial V}$$

$$= -1 + (\epsilon_2 c(t) + \mu)\lambda_8 + \frac{\beta_{VH}p_1 S}{p_1(S+L)+(1-p_1)I}(\lambda_9 - \lambda_{10}), \tag{2.50}$$

$$\frac{d\lambda_9}{dt} = -\frac{\partial H}{\partial S}$$

$$= -\frac{\beta_{HV} IU p_1(1-p_1)(\lambda_7 - \lambda_8)}{[p_1(S+L)+(1-p_1)I]^2} - \frac{\beta_{VH}p_1 V(p_1 L + (1-p_1)I)}{[p_1(S+L)+(1-p_1)I]^2}(\lambda_9 - \lambda_{10})$$

$$- r\left(1 - \frac{2S+L+I}{K_H}\right)\lambda_9 + h\lambda_9, \tag{2.51}$$

$$\frac{d\lambda_{10}}{dt} = -\frac{\partial H}{\partial L}$$

$$= -1 - \frac{\beta_{HV}p_1(1-p_1)IU}{[p_1(S+L)+(1-p_1)I]^2}(\lambda_7 - \lambda_8) + \frac{\beta_{VH}p_1^2 VS}{[p_1(S+L)+(1-p_1)I]^2}(\lambda_9 - \lambda_{10})$$

$$+ \frac{rS}{K_H}\lambda_9 + h\lambda_{10} + \alpha(\lambda_{10} - \lambda_{11}), \tag{2.52}$$

$$\frac{d\lambda_{11}}{dt} = -\frac{\partial H}{\partial I}$$

$$= -1 + \frac{\beta_{HV}(1-p_1)U}{p_1(S+L)+(1-p_1)I}(\lambda_7 - \lambda_8) - \frac{\beta_{HV}(1-p_1)^2 IU}{[p_1(S+L)+(1-p_1)I]^2}(\lambda_7 - \lambda_8)$$

$$+ \frac{\beta_{VH}p_1(1-p_1)VS}{[p_1(S+L)+(1-p_1)I]^2}(\lambda_{10} - \lambda_9) + \frac{rS}{K_H}\lambda_9 + (\epsilon_3 g(t) + h)\lambda_{11}. \tag{2.53}$$

with transversality conditions $\lambda_j(t_f) = 0$. Furthermore, by applying the Pontryagin's maximum Principle and the optimality conditions, we have:

$$\frac{\partial H}{\partial c} = 0, \qquad \text{and,} \qquad \frac{\partial H}{\partial g} = 0. \tag{2.54}$$

Thus, optimal controls are characterized by:

$$c^* = \min\left\{c_{\max}, \max\left\{0, \frac{\epsilon_1(\lambda_2 N_1 + \lambda_3 N_2 + \lambda_4 N_3 + \lambda_5 N_4) + \epsilon_2(\lambda_7 U + \lambda_8 V)}{B_1}\right\}\right\}, \tag{2.55}$$

$$g^* = \min\left\{g_{\max}, \max\left\{0, \frac{\epsilon_3\lambda_{11} I}{B_2}\right\}\right\}, \tag{2.56}$$

where $c_{\max} \leq 1$ and $g_{\max} \leq 1$ are the feasible upper bounds of the controls $c(t)$ and $g(t)$.

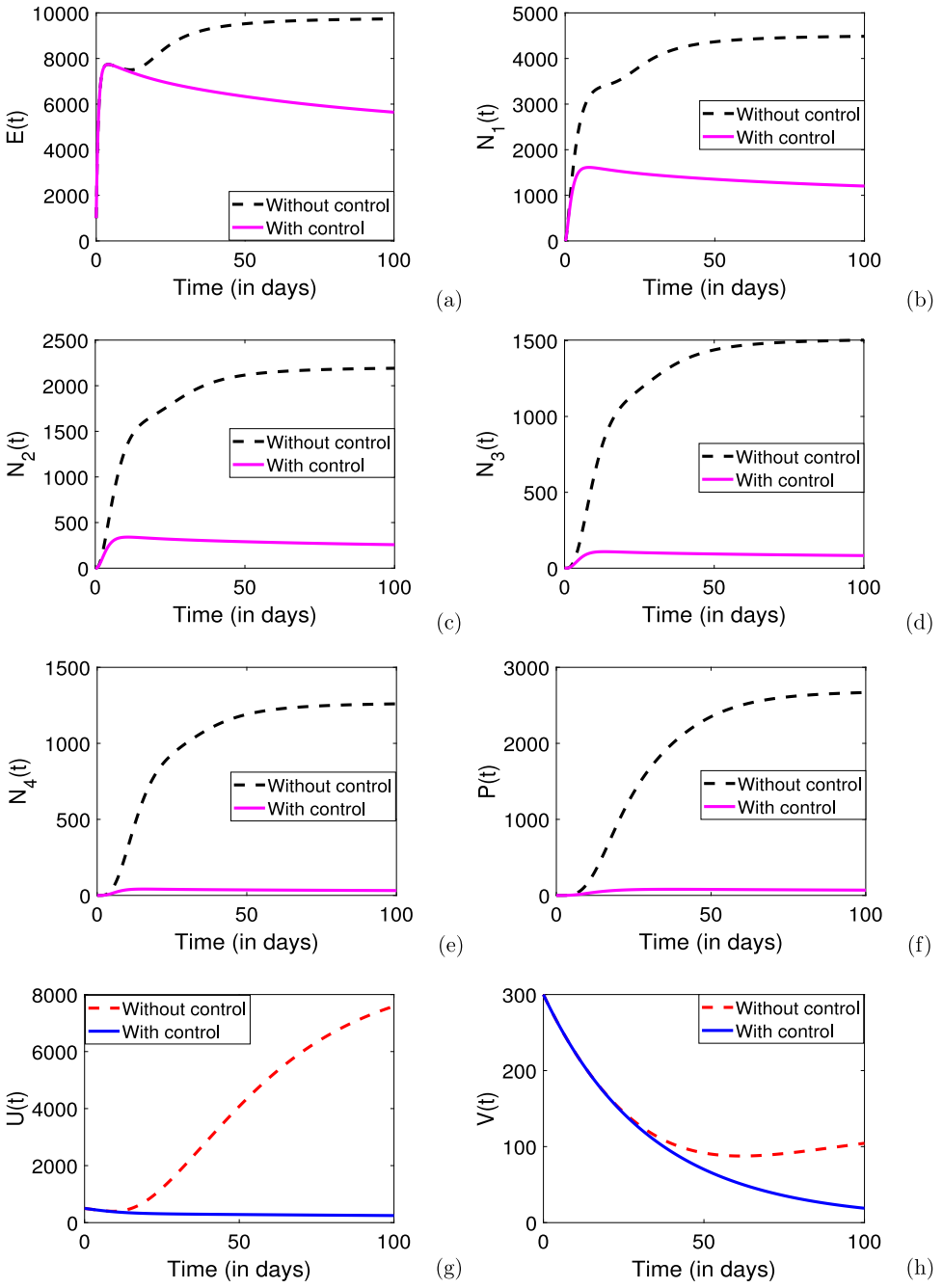

Fig. 6. Simulation results showing the dynamics of immature and adult whitefly population with and without optimal control under strategy A with $B_1 = 0.1$, $B_2 = 0.01$, $\epsilon_1 = 0.8$, $\epsilon_2 = 0$ and $\epsilon_3 = 0.5$.

3. Results and discussions

To determine the strength and effectiveness of the control strategies, we numerically solve the optimal control problem using the forward–backward sweep method [29] with the Runge–Kutta fourth order scheme programmed in Matlab. In our simulations, we set the weight constants A_1 and A_2 to unity, and this implies that the reduction of adult vectors has equivalent importance to the reduction of immature vectors. Furthermore, we assume that use of insecticides is more expensive in comparison to roguing, hence we set $B_1 \geq B_2$. To investigate the effectiveness of the control strategies, we shall compare the implications of varying the efficacy of the control strategies (ϵ_i).

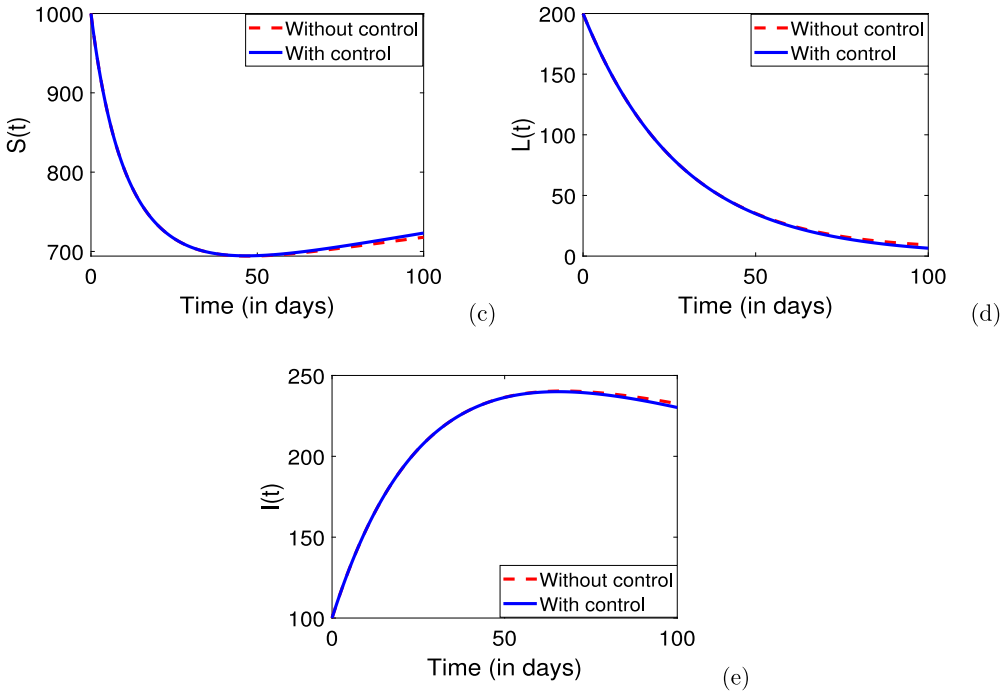

Fig. 7. Simulation results showing the dynamics of adult whitefly and plant population with and without optimal control under strategy A with $B_1 = 0.1$, $B_2 = 0.01$, $\epsilon_1 = 0.8$ $\epsilon_2 = 0$ and $\epsilon_3 = 0.5$.

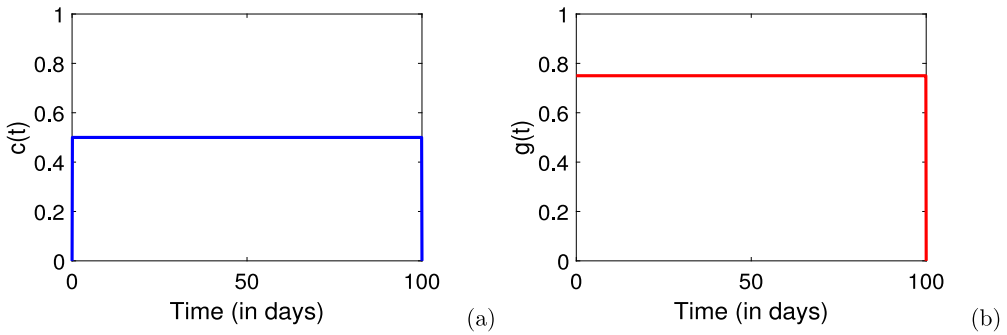

Fig. 8. Plots of the control profiles $c(t)$ and $g(t)$ for strategy A with $B_1 = 0.1$, $B_2 = 0.01$, $\epsilon_1 = 0.8$ $\epsilon_2 = 0$ and $\epsilon_3 = 0.5$.

Figs. 6–8 show a scenario in which the insecticides used by farmers have no effect on the adult whitefly population. For example, when farmers utilize IGR as an intervention strategy, these insecticides are known to be effective against whitefly nymphs but not on adult population [3]. As we can observe, implementing time dependent controls strategies will significantly reduce vector populations (both immature and adult) compared to non-time-dependent control strategies but this will not result in the extinction of the vector population. We can also note that this approach may not result in significant changes in the host populations (Fig. 7). Moreover, to achieve these results, all control efforts need to be maintained at their maximum intensity throughout the time horizon (Fig. 8).

To quantify disease dynamics when insecticides are effective to both immature and mature whitefly population, we simulated model (2.30)–(2.40) with $0 < \epsilon_1 < 1$, and $0 < \epsilon_2 < 1$, and the output is presented in Figs. 9–11. Without loss of generality, we set $\epsilon_1 = \epsilon_2 = 0.8$, and $\epsilon_3 = 0.5$. As we can observe, the findings show that when insecticides are effective at reducing both the immature and adult whitefly population, time-dependent control efforts will lead to the extinction of vectors (both immature and adult population) and infectious plants. As has been shown, this outcome will be attained if the control efforts are maintained at their maximum intensity for the entire time horizon. To further quantify the impact of the effectiveness of the control strategies on the population dynamics of the host and vector, we simulated model (2.30)–(2.40) on two levels of effectiveness: low ($\epsilon_1 = \epsilon_2 = \epsilon_3 = 40\%$) and high ($\epsilon_1 = \epsilon_2 = \epsilon_3 = 80\%$) and the output is presented in Figs. 12 and Fig. 13. As highlighted in earlier

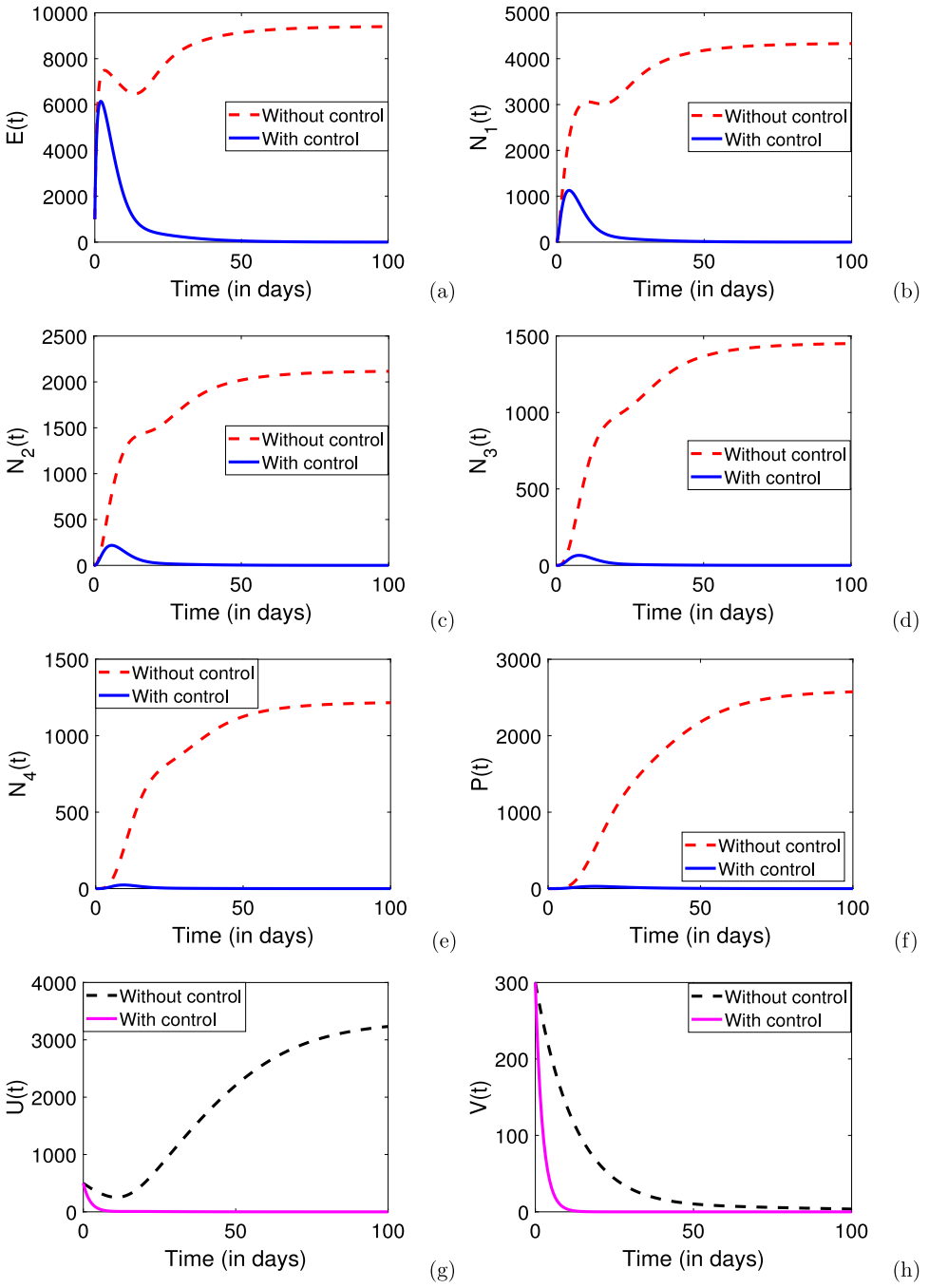

Fig. 9. Simulation results showing the dynamics of immature whitefly population with and without optimal control under strategy A with $B_1 = 0.1$, $B_2 = 0.01$, $\epsilon_1 = \epsilon_2 = 0.8$ and $\epsilon_3 = 0.5$.

optimal control results, we can also observe that when the effectiveness of control strategies is relatively high, the vector population decreases significantly and may become extinct after 50 days of implementing the controls. These results reinforce the argument that effectiveness of control strategies is of utmost importance on controlling the spread of CMD.

4. Concluding remarks

We proposed a plant-vector-virus model of CMD that incorporates all known immature stages of the whitefly, vector feeding behavior and control strategies, to understand the disease dynamics and the impact control strategies. Prior studies have shown that

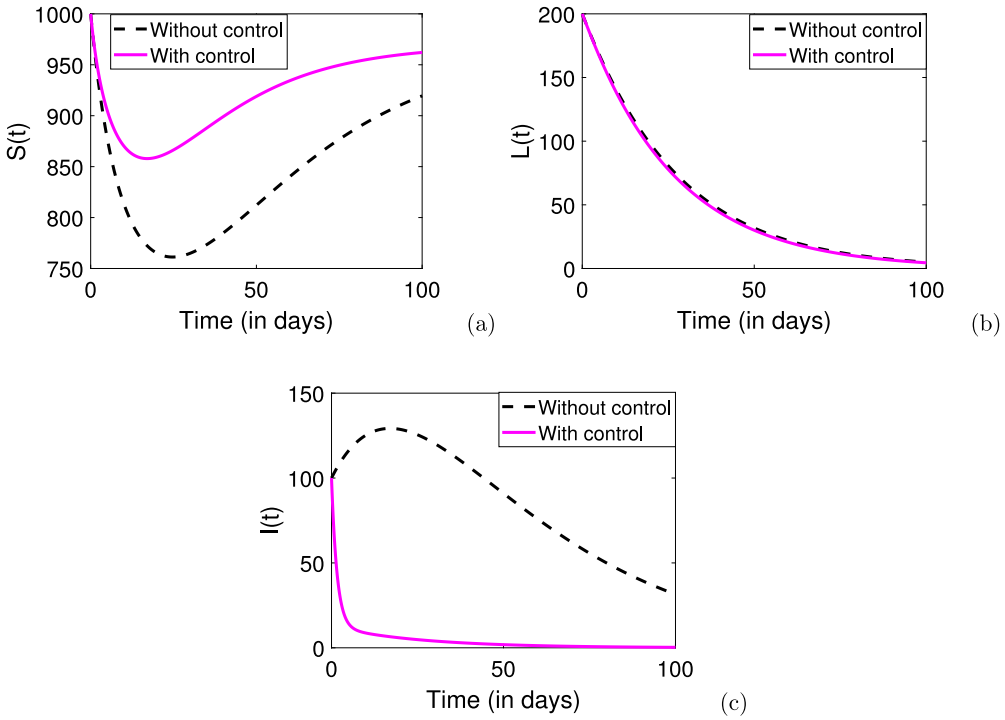

Fig. 10. Simulation results showing the dynamics of adult whitefly and plant population with and without optimal control under strategy A with $B_1 = 0.1$, $B_2 = 0.01$, $\epsilon_1 = \epsilon_2 = 0.8$ and $\epsilon_3 = 0.5$.

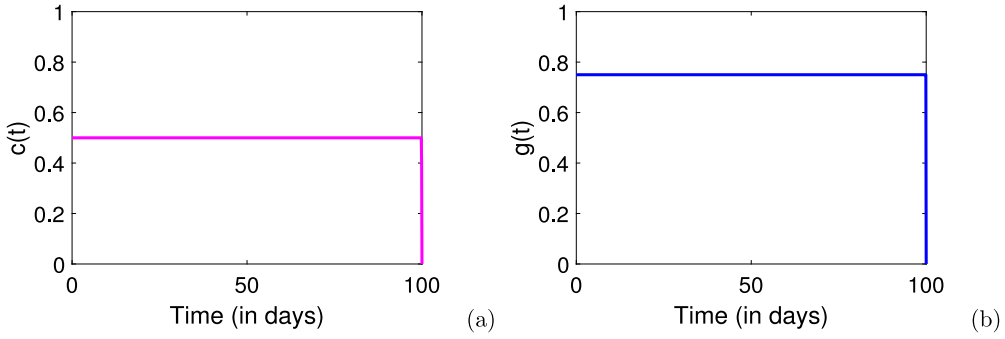

Fig. 11. Plots of the control profiles $c(t)$ and $g(t)$ for strategy A with $B_1 = 0.1$, $B_2 = 0.01$, $\epsilon_1 = \epsilon_2 = 0.8$ and $\epsilon_3 = 0.5$.

the preference of vector settlement for the infected or healthy host significantly impacts the disease transmission dynamics [17]. Hence, this aspect needs to be integrated in host-vector-virus models. We commence by investigating the growth dynamics of the whitefly population. Thus, we proposed a mathematical framework that fully tracks the life cycle of the whitefly population from egg to adult stages. We included all the four instar stages and the pupa stage since the probability of survival and development varies from one stage to another. In particular, it is well known that first instars are highly mobile during the first few hours after egg hatching making them more vulnerable to environmental stress factors [18]. From the whitefly growth model, we established a threshold parameter, the offspring number which gives the average number of new offsprings an adult female whitefly is capable of producing in its entire lifespan. In other words, the offspring number measures the power of the whitefly population to persist. We performed the sensitivity analysis of the offspring number to identify the model parameters that have a strong influence on its growth or decrease. The findings showed that an increase in the oviposition of the adult whitefly significantly increases the growth of the whitefly population. In contrast, we observed that an increase in mortality rates, particularly at the adult stage, significantly reduces the persistence of whitefly population.

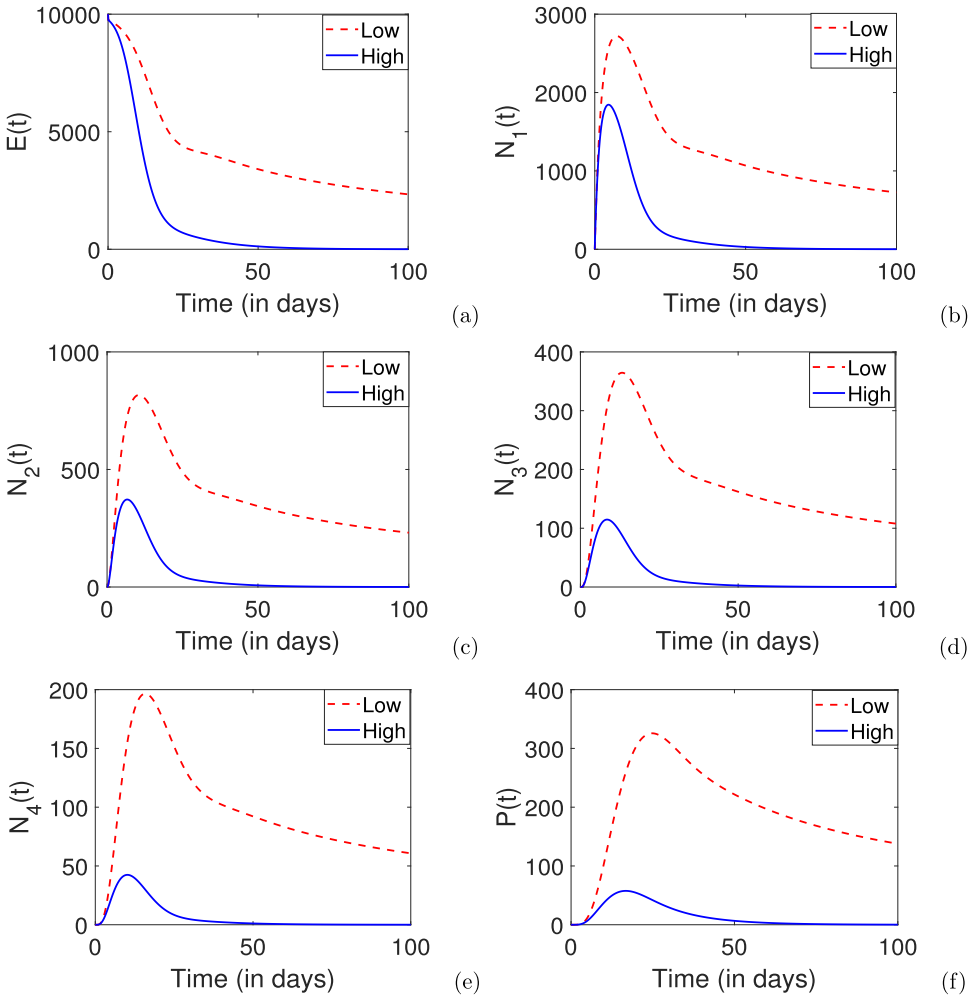

Fig. 12. Simulation results showing the dynamics of immature whitefly population with low ($\epsilon_1 = \epsilon_2 = \epsilon_3 = 40\%$) and high ($\epsilon_1 = \epsilon_2 = \epsilon_3 = 80\%$) efficient controls.

We extended the whitefly growth model to incorporate the host and virus transmission-influenced by vector feeding behavior. We derived the reproduction number ($\mathcal{R}_0$)-a metric for measuring the power of the disease to invade the population. We observed that the reproduction number strongly depends on the offspring number. If the offspring number is less than unity, then the disease will die out due to the extinction of the whitefly population. In contrast, an increase of the offspring number significantly increases disease transmission potential. We carried out a bifurcation analysis and observed a forward bifurcation at $\mathcal{R}_0 = 1$. We then extended the host-vector-virus model to incorporate time-dependent insecticide and roguing efforts. Exploring various ways of implementing the aforementioned control strategies revealed that the best outcome will be achieved whenever the controls are implemented in combination and at maximum possible efficiency. The findings from this study demonstrate the importance of the interplay between vector feeding behavior and control strategies in disease dynamics.

Our study only predicted the impact of insecticide and plant roguing on CMD dynamics, however, there is a growing interest among researchers to establish the significance of biological control programs in controlling disease prevalence. Of particular importance is the fact that biocontrol has the potential to control the pest at the threshold level in an eco-friendly way and make a sustainable environment without affecting fauna and flora [30]. Hence, in future we hope to extend the proposed framework to incorporate biological control strategies. Additionally, although mathematical models have made considerable contributions in predicting disease dynamics in the human population and agricultural realm, it is essential for these to be validated with experimental data so that the proposed model(s) will yield a reasonably accurate prediction. Due to the scarcity of experimental data we were not able to validate our study with experimental data, however, in future we aim to work with researchers who have the necessary data. With reliable datasets we will enhance the applicability of our work.

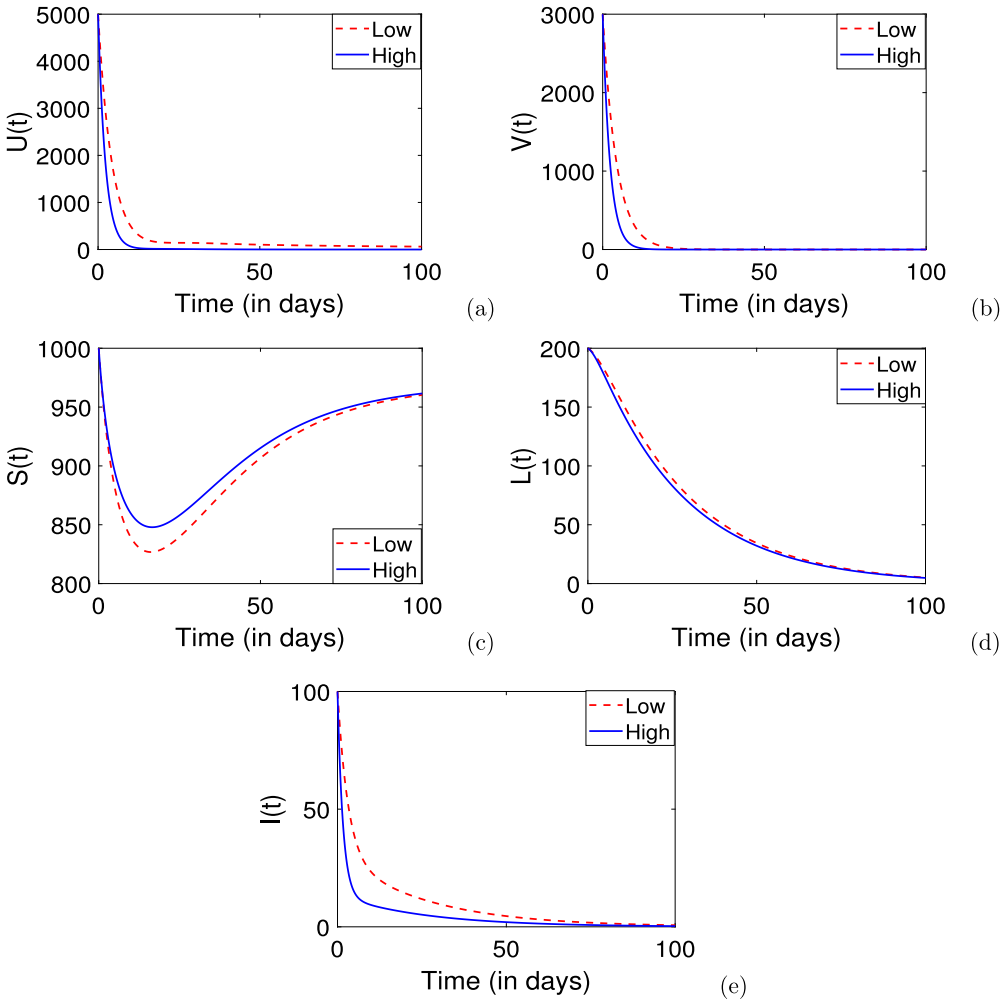

Fig. 13. Simulation results showing the dynamics of adult whitefly and plant population with low ($\epsilon_1 = \epsilon_2 = \epsilon_3 = 40\%$) and high ($\epsilon_1 = \epsilon_2 = \epsilon_3 = 80\%$) efficient controls.

Declaration of competing interest

The authors declare that they have no known competing financial or personal relationships that could have appeared to influence the work reported in this study.

Acknowledgments

The authors would like to thank the anonymous reviewers for their valuable comments and suggestions.

Funding

No funding was received to carry out this study.

Data availability

No data was used for the research described in the article.

References

[1] Adebayo WG. Cassava production in Africa: A panel analysis of the drivers and trends. Heliyon 2023;9(9).
[2] Burns A, Gleadow R, Cliff J, Zacarias A, Cavagnaro T. Cassava: The drought, war and famine crop in a changing world. Sustainability 2010;2(11):3572–607.
[3] Perring TM, Stansly PA, Liu TX, Smith HA, Andreason SA. Whiteflies: Biology, ecology, and management. In: Sustainable management of arthropod pests of tomato. Academic Press; 2018, p. 73–110.
[4] Sikazwe G, Yocgo RE, Landi P, Richardson DM, Hui C. Managing whitefly development to control cassava brown streak virus coinfections. Ecol Model 2024;493:110753.
[5] Adhurya S, Basir FA, Ray S. Stage-structure model for the dynamics of whitefly transmitted plant viral disease: An optimal control approach. Comput Appl Math 2022;41(4):154.
[6] Chan MS, Jeger MJ. An analytical model of plant virus disease dynamics with roguing and replanting. J Appl Ecol 1994;413–27.
[7] Gao S, Xia L, Liu Y, Xie D. A plant virus disease model with periodic environment and pulse roguing. Stud Appl Math 2016;136(4):357–81.
[8] Bokil VA, Allen LJS, Jeger MJ, Lenhart S. Optimal control of a vectored plant disease model for a crop with continuous replanting. J Biol Dyn 2019;13(sup1):325–53.
[9] Hamelin FM, Bowen B, Bernhard P, Bokil VA. Optimal control of plant disease epidemics with clean seed usage. Bull Math Biol 2021;83:1–24.
[10] Al Basir F, Ray S. Impact of farming awareness based roguing, insecticide spraying and optimal control on the dynamics of mosaic disease. Ric Mat 2020;69(2):393–412.
[11] Al Basir F, Blyuss KB, Ray S. Modelling the effects of awareness-based interventions to control the mosaic disease of Jatropha curcas. Ecol Complex 2018;36:92–100.
[12] Abraha T, Al Basir F, Obsu LL, Torres DF. Pest control using farming awareness: Impact of time delays and optimal use of biopesticides. Chaos Solitons Fractals 2021;146:110869.
[13] Rakshit N, Al Basir F, Banerjee A, Ray S. Dynamics of plant mosaic disease propagation and the usefulness of roguing as an alternative biological control. Ecol Complex 2019;38:15–23.
[14] McQuaid CF, Gilligan CA, van den Bosch F. Considering behaviour to ensure the success of a disease control strategy. R Soc Open Sci 2017;4(12):170721.
[15] Holt J, Jeger MJ, Thresh JM, Otim-Nape GW. An epidemilogical model incorporating vector population dynamics applied to African cassava mosaic virus disease. J Appl Ecol 1997;793–806.
[16] Su M, Yang K. Effects of predator modulation and vector preference on pathogen transmission in plant populations. Biosystems 2022;222:104794.
[17] Shoemaker LG, Hayhurst E, Weiss-Lehman CP, Strauss AT, Porath-Krause A, Borer ET, et al. Pathogens manipulate the preference of vectors, slowing disease spread in a multi-host system. Ecol Lett 2019;22(7):1115–25.
[18] Aregbesola OZ, Legg JP, Lund OS, Sigsgaard L, Sporleder M, Carhuapoma P, et al. Life history and temperature-dependence of cassava-colonising populations of Bemisia tabaci. J Pest Sci 2020;93:1225–41.
[19] Sani I, Ismail SI, Abdullah S, Jalinas J, Jamian S, Saad N. A review of the biology and control of whitefly, bemisia tabaci (Hemiptera: Aleyrodidae), with special reference to biological control using entomopathogenic fungi. Insects 2020;11(9):619.
[20] Kumarasinghe NC, Salim N, Wijayarathne W. Identification and biology of two whitefly species on cassava in Sri Lanka. J Plant Prot Res 2009;49(4).
[21] Gao S, Martcheva M, Miao H, Rong L. A two-sex model of human papillomavirus infection: Vaccination strategies and a case study. J Theoret Biol 2022;536:111006.
[22] Asiimwe P, Ecaat JS, Otim M, Gerling D, Kyamanywa S, Legg JP. Life-table analysis of mortality factors affecting populations of bemisia tabaci on cassava in uganda. Èntomol Exp Appl 2007;122(1):37–44.
[23] Macfadyen S, Paull C, Boykin LM, De Barro P, Maruthi MN, Otim M, et al. Cassava whitefly, Bemisia tabaci (Gennadius)(Hemiptera: Aleyrodidae) in East African farming landscapes: A review of the factors determining abundance. Bull Entomol Res 2018;108(5):565–82.
[24] Thresh JM, Otim-Nape GW, Thankappan M, Muniyappa V. The mosaic diseases of cassava in Africa and India caused by whitefly-borne geminiviruses. 1998.
[25] Njoroge MK, Mutisya DL, Miano DW, Kilalo DC. Whitefly species efficiency in transmitting cassava mosaic and brown streak virus diseases. Cogent Biol 2017;3(1):1311499.
[26] van den Driessche P, Watmough J. Reproduction number and subthreshold endemic equilibria for compartment models of disease transmission. Math Biosci 2002;180:29–48.
[27] Castillo-Chavez C, Song B. Dynamical models of tuberculosis and their applications. Math Biosci Eng 2004;1(2):361–404.
[28] Pontryagin LS, Boltyanskii VT, Gamkrelidze RV, Mishcheuko EF. The mathematical theory of optimal processes. New Jersey: Wiley; 1962.
[29] Lenhart S, Workman JT. Optimal control applied to biological models. London: Chapman and Hall/CRC; 2007.
[30] Tariq M, Khan A, Asif M, Khan F, Ansari T, Shariq M, et al. Biological control: A sustainable and practical approach for plant disease management. Acta Agric Scand Sect B 2020;70(6):507–24.